acta physica slovaca vol. 52 No. 2, 55 – 64 **April 2002**

ASSESSMENT OF SENSITIVITY AND RESOLUTION LIMITS OF SCANNING CAPACITANCE MICROSCOPES

Š. Lányi[1]
Institute of Physics, Slovak Academy of Sciences, Dúbravská cesta 9, SK 842 28 Bratislava, Slovakia

Received 17 September 2001, in final form 13 February 2002, accepted 14 February 2002

Based on analysis of noise limited sensitivity of different capacitance detection methods, the achievable lateral resolution of Scanning Capacitance Microscopes has been estimated. The ultimate sensitivity is below 3×10^{-21} F/$\sqrt{\text{Hz}}$/V. A lateral resolution of about 2 nm is expected with probes with 7-nm radius of curvature. About 5 nm has been already achieved with a tip radius of approximately 25 nm. Improving the signal-to-noise ratio using larger applied voltage than a few volts must lead to degradation of lateral resolution, since the tip-to-sample distance has to be increased to prevent voltage breakdown or excessive tunnelling to occur.

PACS: 68.35.Bs, 77.55.+f, 07.79.-v, 07.50.Hg, 41.20.Cv

1 Introduction

Scanning Capacitance Microscopes (SCM) [1–4] are becoming interesting tools for imaging the morphology and analysis of structures on the surface of conductors, either free or coated with insulating films, and of buried structures in semiconductors and dielectrics. They are considered as most promising to fulfil the requirements of semiconductor industries for the analysis of next generation of integrated circuits [5]. The most representative applications comprise the nanometre-scale analysis of free carrier concentration in semiconductors [6] or the delineation of *pn* junctions in integrated circuits [7].

The SCM uses a sharp conducting tip situated in the proximity of a conducting surface, or a conducting substrate covered by a thin insulator, as a probe. Between the tip apex and the conducting substrate a small capacitor is formed. Its capacitance depends besides on the geometry also on the dielectric constant of the material between the electrodes. By raster scanning the probe, an image of surface topography or of the topography modified by local changes of dielectric constant can be obtained.

The capacitance detection principles applied in microscopes can be divided into three groups. The most popular is the use of the RCA CED VideoDisc pickup. It contains a microstrip resonator, coupled to an oscillator oscillating at 915 MHz, a frequency on the flank of the resonant

[1] E-mail address: fyzilyis@savba.sk

0323-0465/02 © Institute of Physics, SAS, Bratislava, Slovakia

curve of the resonator. The frequency of resonance is fine-tuned by the tip/sample capacitance, modulating the RF voltage in the resonator [8]. A similar approach based on lumped element circuits was employed in paper [1] at 90 MHz. A different concept was introduced by Lányi and co-workers [4]. They measured the ac current flowing through the tip/sample capacitance at 2 MHz phase sensitively, with the possibility to separate the real and imaginary (loss) components of the capacitance. The third principally different method is based on measuring the electrostatic force between the sample and a cantilever, to which a dc or ac voltage is connected [9]. A modulation of the probe/sample spacing produces a force component proportional to the derivative of the capacitance and to the square of the applied voltage.

The lateral resolution of capacitance microscopes was usually deduced experimentally, from resolved features in images. In [1] a resolution of 1.5 μm and in [2] 200 nm laterally and 5 nm perpendicularly to the surface was achieved. Williams [3] pushed the resolution limit to 25 nm and Lányi [4] to 10 nm. Kleinknecht and co-workers [2] concluded that the limit for resolution be 7 nm laterally and 1 nm vertically. However, their analysis is based on somewhat problematic assumptions. They approximated the tip by a sphere, what underestimates the capacitance of the probe [10]. They assumed a minimal probe-to-sample separation of 1 nm, a value too small because of onset of tunnelling current, and they assumed that the resolution would roughly correspond to the tip diameter.

The radial dependence of sensitivity of probes with realistic geometry was analysed by Lányi et al. using the Finite Element Method [10,11]. They have found that a ratio of tip-radius-to-separation of approximately 5 yields the optimum of resolution and signal-to-noise ratio and that the resolution cannot be uniquely determined without the concept of contrast, to which it is related. Reducing the radius of the tip apex alone decreases the signal-to-noise ratio and the contrast but does not improve the resolution. The wide range of the electrostatic interaction causes distortion of surface features [12] and imaging of deep trenches and holes represent serious problems.

An important issue in optimising the probe shape and operating conditions for the best resolution is the achievable sensitivity of capacitance detection at an acceptable voltage between the probe and the sample. This must be small enough to prevent voltage breakdown or flow of excessive tunnelling current. Large applied voltage would require large probe-to-sample distance and deterioration of the radius-to-separation ratio, hence degradation of lateral resolution. The goal of the present communication is to analyse the limits of SCM from this point of view.

2 The noise of capacitance sensors

The sensitivity of electrostatic-force-based capacitance detection was analysed in [9] and we shall only comment it later. The capacitance is usually measured by means of bridges, instruments based on tuned circuits, or measuring phase-sensitively the capacitive current. We shall focus on their possibilities. A bridge circuit was not yet used in a SCM, nevertheless, it is the most frequently used capacitance measurement principle. For measurement of capacitances in the pF-range also various switched capacitor methods were applied [13]. They are robust, well suited to industrial environment but too slow and not sensitive enough to resolve minute capacitance changes required by SCM.

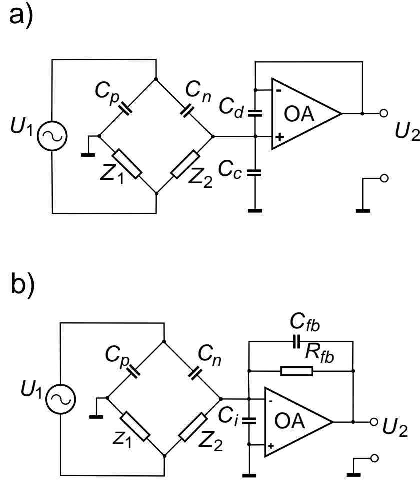

Fig. 1. Bridge circuit with a buffer a) and current-to-voltage converter b) as output amplifier.

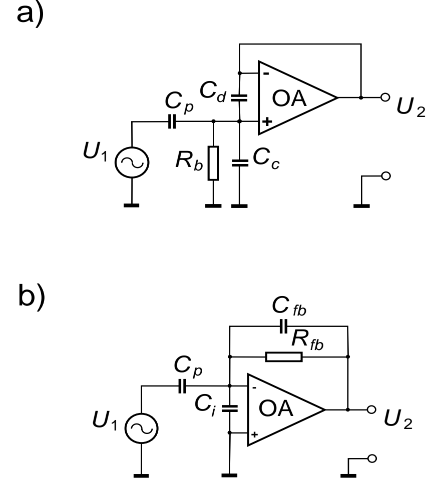

Fig. 2. Current measurement with a buffer a) and current-to-voltage converter b).

The basic bridge circuits, that could be used in a SCM, are shown in Fig. 1, in a) in connection with a high-input-impedance buffer stage, whereas in b) the bridge unbalance is sensed by means of a current-to-voltage converter (IUC). C_p is the probe-to-sample capacitance. An advantage of a bridge would be the possibility to balance out relatively large parasitic capacitances of the probe, connecting wires or cables, etc., at the same time pertaining high stability. The highest sensitivity of a bridge is achieved if the voltages in its branches are approximately equal. Since C_p is small, Z_1 should be a high impedance. Were Z_1 and Z_2 capacitors, a dc path biasing the input of the buffer would be needed. The ac generator is assumed floating to avoid the need of differential sensing amplifiers. From the point of view of noise the bridge can be reduced to circuits directly measuring the capacitive current, seen in Fig. 2.

A direct phase-sensitive measurement of the current flowing through the SCM probe that is high-impedance, can be performed using similar amlifiers as to the sensing of the bridge unbalance, followed by a lock-in amplifier or other phase-sensitive detector. The noise of unity gain buffers and IUCs with low input capacitance has been analysed in [14]. C_c, the common-mode input capacitance of the op-amp, connected to a high impedance source, seriously limits the achievable bandwidth unless it is suppressed by bootstrap of supply rails (not shown in Fig. 2) [15]. Under optimal conditions, the dominant source of noise is the thermal noise of the source and/or biasing resistor. To achieve a high transimpedance in IUC large feedback resistor R_{fb} and the smallest possible parasitic capacitance C_{fb} is required. The signal-to-noise-spectral-density of the buffer becomes

$$S/Nsd = U_1/\sqrt{e_n^2 + i_n^2 Z^2 + 4kTZ^2/R_b}\,, \tag{1}$$

where e_n is the op-amp noise voltage spectral density, i_n the noise current spectral density, Z

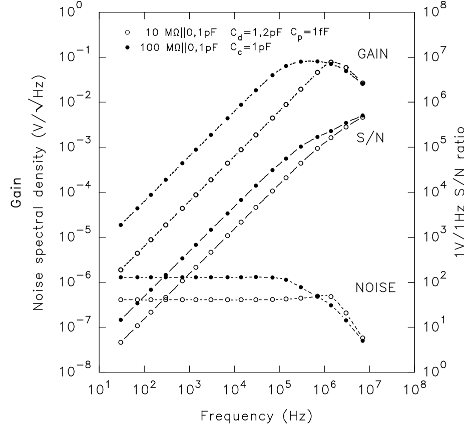

Fig. 3. Gain, noise spectral density and S/N ratio of a buffer with bootstrapped supply nodes.

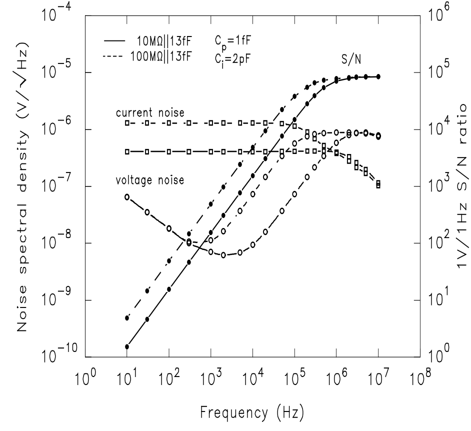

Fig. 4. Spectral densities of noise current and noise voltage and S/N ratio of a current-to-voltage converter.

the signal source impedance, R_b the dc biasing resistance, k the Boltzmann constant and T temperature. At higher frequencies, the parasitic capacitance of R_b, neglected for simplicity in (1), must be also considered. The highest signal-to-noise ratio of the buffer is achieved with large R_b, up to 0,1 to 1 GΩ if it can be used. The computed gain, noise spectral density and signal-to-noise ratio of a buffer utilising a bootstrapped fast FET-input op-amp (OPA655 from Burr-Brown), connected to a 1 fF capacitor representing the probe, is seen in Fig. 3.

The S/Nsd of a current-to-voltage converter is

$$S/Nsd = U_1/\sqrt{e_n^2\left(1 + Z/R_{fb} + Z/X_i\right)^2 + i_n^2 Z^2 + 4kTZ^2/R_{fb}}\,, \tag{2}$$

where X_i denotes the reactance of the op-amp input capacitance $C_i = C_d + C_c/2$. Here again, at higher frequencies C_{fb}, the parasitic capacitance between the output and the non-inverting input bypassing R_{fb}, must be taken into account. The lowest noise is achieved with large R_{fb}, however, the op-amp input capacitance may reduce the signal-to-noise ratio by orders of magnitude [14]. Fig. 4 shows the signal-to-noise ratio and the input current and voltage noise spectral densities of a current-to-voltage converter, using a composite op-amp (with an OPA655 at the input) to reduce the parasitic capacitance between the output and the inverting input (cf. Fig. 5). Evident is a large increase of the voltage noise that limits the S/N ratio.

The resonance-based measurement is illustrated by Fig. 6. The noise of a parallel resonant circuit corresponds to the thermal noise of the real part of its impedance. The impedance can be expressed as

$$|Z_{LC}| = |R_d/(1 + jQF)| = R_d/\sqrt{(1 + Q^2F^2)}\,, \tag{3}$$

where Q is the quality, R_d the impedance at the frequency of resonancef_r and $F = \Delta f/f_r$. Since it does not operate at resonance but rather at slightly higher frequency of the oscillator f_o,

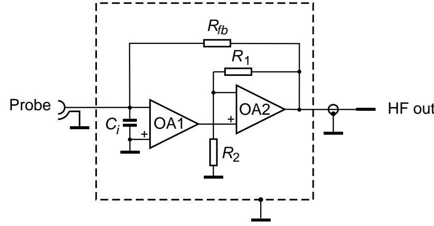

Fig. 5. Simplified circuit diagram of the composite current-to-voltage follower.

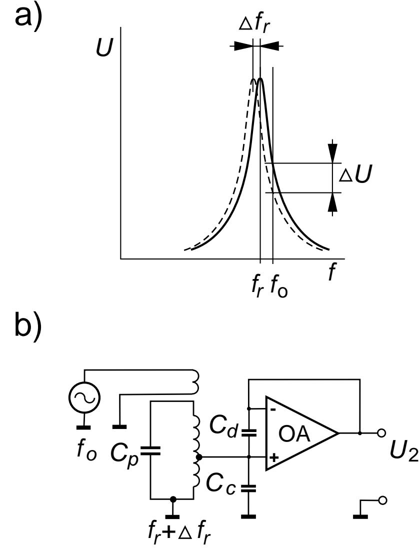

Fig. 6. Principle a) and simplified circuit diagram b) of resonant-circuit-based measurement of the capacitance.

at which the signal is about 6 dB below the maximum, $\Delta f = f_o - f_r$ and the effective resistance will be

$$R = Re|Z_{LC} = R_d/(1 + Q^2F^2)\,. \tag{4}$$

The thermal noise voltage spectral density of a resistor R is $e_n = \sqrt{(4kTR)}$, thus from expressions (3) and (4) results that the signal-to-noise-spectral-density ratio of the resonant circuit does not change if it is slightly out of resonance. We arrive to

$$S/Nsd = U_1/\sqrt{4kTR_d}\,, \tag{5}$$

where U_1 is the voltage at resonance. Though the integral noise of the resonant circuit remains unaltered, the resulting noise is reduced by subsequent low-pass filtering the dc output (cf. Fig. 7). The change of the resonant frequency $f_r = [2\pi\sqrt{(LC)}]^{-1}$ caused by a small change of the capacitance is $\mathrm{d}f_r/\mathrm{d}C = 0.5 f_r/C$. Therefore, for high sensitivity the parasitic capacitance, including also that of the coil, must be as small as possible. Values about 1 pF might be achievable. This limits the choice of the inductance to at most a few μH and the operating frequency to about 50 to 200 MHz. For constant Q the impedance at resonance $R_d \sim 1/f_r$, hence the signal-to-noise ratio $S/Nsd \sim \sqrt{f}$. At lower frequencies the increase of circuit's capacitance C reduces the frequency sensitivity and leads to rapid fall of S/N ratio.

At higher frequencies, distributed element circuits are used. Although the resonant circuit is then replaced by a (stripline or other) resonator, the conclusions would be similar, except that the frequency sensitivity $\mathrm{d}f_r/\mathrm{d}C$ is $(0.05 \div 0.1) f_r/C$ [8].

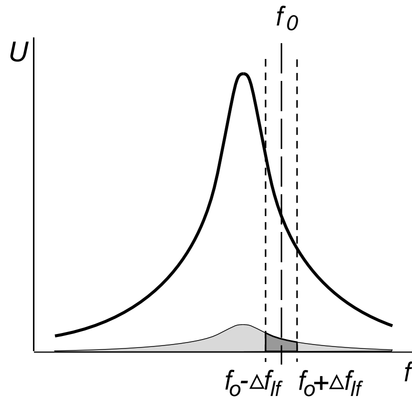

Fig. 7. Origin of noise at the low-frequency output of a resonant-circuit-based sensor.

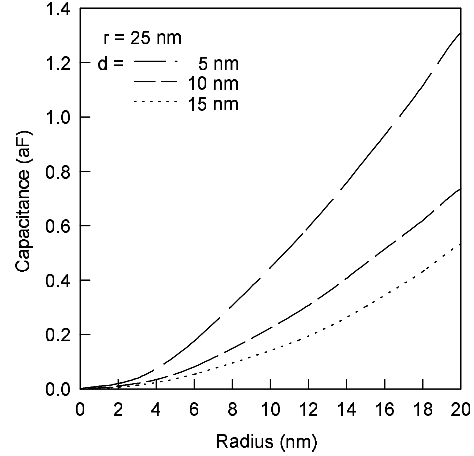

Fig. 8. Radial dependence of the capacitance of a SCM probe.

The capacitance of the probe, as it scans over a not perfectly flat surface, would change, introducing certain amplitude modulation of the measuring signal. Since the achievable lateral resolution is approximately inversely proportional to the probe-to-sample distance, the microscope is usually operated in such a mode that keeps it constant by modifying the probe position by a feedback. The quantity used to create an image is either the capacitance change or the feedback voltage. In either case a certain frequency bandwidth is required after turning the signal to a low-frequency voltage. The demodulation passes the noise of two side-bands to the output. Therefore, the signal-to-noise ratio resulting from expressions (1), (2) and (5) is reduced by 3 dB. The resulting noise is obtained by integration over the low-frequency band. Since the measuring frequency is much higher than the usually required bandwidth B, a frequency dependence of the noise spectral density can be ignored and $S/N = S/(Nsd\sqrt{B})$.

3 The sensitivity of capacitance sensors

The sensitivity of the circuits will be determined as the smallest detectable capacitance at 1V applied to the probe capacitance C_p, in 1-kHz-noise band. The possibility to compensate the parasitic capacitance by a bridge is only an apparent advantage. Large C_p would require a smaller Z_1 that would reduce the sensitivity and the S/N ratio. Therefore, the sensitivity that could be achieved with a bridge is at the best that of direct measurement of the current, or worse.

The impedance at resonance of the parallel LC circuit has been calculated for $Q = 100$ and $C = 1$ pF. In accord with [8], the characteristic impedance of the strip-line resonator, quality Q and stray capacitance were assumed 275 Ω 45 and 0.1 pF, respectively. The obtained results are summarised in Table 1.

frequency [MHz]	buffer	IUC	lumped LC	distributed LC
1	2.3×10^{-19}	6.9×10^{-19}		
3	1.3×10^{-19}	6.5×10^{-19}		
10	7.4×10^{-20}	7.1×10^{-19}		
50			$1.1 \times 10^{-19\,*}$	
200			$5.7 \times 10^{-20\,*}$	
900				$1.4 \times 10^{-20\,*}$ $2.5 \times 10^{-20\,\dagger}$ $3.5 \times 10^{-19\,\ddagger}$

*Noise limit
†Sensitivity of RCA CED VideoDisc pickup
‡Highest of reported sensitivities

Tab. 1. Capacitance sensitivity (F/V) in 1-kHz bandwidth

4 The limiting resolution

The radial sensitivity of probes with different shapes has been derived using FEM analysis in [4,10–12]. The radial dependence of the stray capacitance of a shielded conical tip with spherical apex and radius of curvature $r = 25\,\text{nm}$, and probe/sample separations $d = 5, 10$ and 15 nm, is seen in Fig. 8. The whole stray capacitance was found to be 320 aF. The stray capacitance of unshielded microfabricated probes is usually larger. The radius ρ of a circular surface area of a flat sample at $d = 5\,\text{nm}$, yielding a capacitance of 1 aF, is 17 nm. This capacitance is larger than the sensitivity of an IUC-based microscope and more than one order of magnitude larger than the resolution of a buffer-based microscope at 1 V in a 1-kHz band. The contrast thus obtained on this length-scale is 1/320, well above the resolution of the electronics (usually 12 to 16 bits, i.e. 1/4095 to 1/65535). Assuming the sensitivity of the buffer-based sensor at 10 MHz and allowing for a S/N ratio 5, the measurable capacitance would be 3.7×10^{-19} F, corresponding to $\rho \approx 10\,\text{nm}$ at contrast reduced to 1/865. An example with even better resolution can be seen in Fig. 9. If the tip radius and the distance are scaled with r, the local contribution to the capacitance is proportional to r. In such arrangement the measurable capacitance would correspond to $\rho = 6.3\,\text{nm}$ at $r = 9.3\,\text{nm}$ and $d = 1.85\,\text{nm}$, with contrast 1/320. Though this distance is typical for tunnelling experiments, these values seem realistic, provided the tunnelling current would not obscure the capacitance measurement, i.e. probably with phase sensitive measurement of the capacitive current or at sufficiently high frequencies. The reserve in resolution of the electronics would make utilisation of lower contrast possible and even allow some increase of the distance d, or reduction of applied voltage.

5 Discussion

The sensitivities marked by asterisk in Table 1 may be affected by the noise of connected circuits, viz. oscillator frequency instability and amplifier noise. The buffer and IUC may operate with

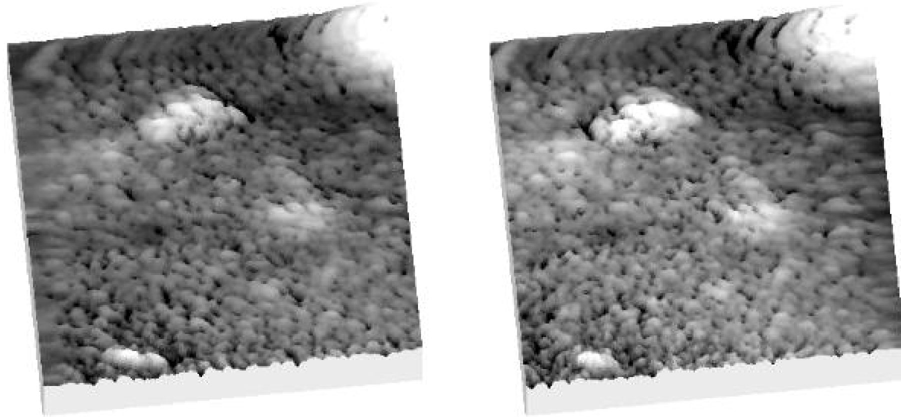

Fig. 9. SCM image of vacuum deposited gold film on silicon (180 nm × 180 nm). Left image scanned from top left to bottom right, right image from top right to bottom left. Features approximately 5 to 10 nm large can be distinguished and correlated in the two images.

such circuit elements that the thermal noise dominates, and any added noise of further circuits is negligible. Their further advantage is that they are not sensitive to frequency, they measure the absolute capacitance and can image also dielectric losses [17]. From Fig. 4 we could deduce that a buffer could be eventually used and yield even somewhat better results at higher frequencies, however, probably at lower and less convenient gain, at which the noise of subsequent circuits could be important. The application of faster low-noise bipolar-input op-amps would not improve the situation, since their input capacitance and open loop gain are comparable to those of the assumed FET-input op-amp but their current noise is usually at least one order of magnitude larger.

Data on the sensitivity or noise of scanning capacitance microscopes are rather scarce. The assumed 1 pF parasitic capacitance of the lumped LC circuit is probably too optimistic, since in paper [1] at 90 MHz 3 pF was achieved. The authors claim a sensitivity 3×10^{-20} F at 1 V in 1-kHz band, whereas our prediction would be at the best 8.5×10^{-20} F/V. The only detailed analysis is of the noise of the RCA CED VideoDisc circuit [8]. The reported noise spectral density corresponded at 5 $\mathrm{V_{max}}$ applied voltage to 2.3×10^{-22} F/$\sqrt{\mathrm{Hz}}$ or 2.5×10^{-20} F/V in a 1-kHz band. This result seems to be realistic since the noise of the resonator alone would be 1.3×10^{-23} F/$\sqrt{\mathrm{Hz}}$ (1.4×10^{-20} F/V). Comparable high sensitivity was not achieved in microscopes. Williams *et al.* [3] claimed a resolution 1×10^{-19} F in a 1-kHz band, probably at 3.5 $\mathrm{V_{rms}}$ (3.5×10^{-19} F/V). Kleinknecht *et al.* [2] estimated the sensitivity to 2×10^{-19} F without specifying the frequency band, and Li *et al.* [18] 5×10^{-19} F in a 100-Hz band (5.5×10^{-18} F/V). The significantly lower sensitivity than that of the videodisk player can be explained by the presence of larger parasitic capacitance (1 pF in paper [2]). On the other hand, the original application of the videodisk pickup required a wide bandwidth, not needed in SCM. The Q of the resonator could be increased, thus improving further the signal-to-noise ratio. A step in this direction was

undertaken recently by Tran *et al.* [19]. They claim to achieve a sensitivity 0.95×10^{-21} F/$\sqrt{\mathrm{Hz}}$ with $0.3\,\mathrm{V_{p-p}}$ sense voltage at the probe, using a sensor similar to the videodisk pickup. However, they evidently ignored the noise of the resonator and related the output voltage to the noise of a low-noise preamplifier. Though they did not give the characteristic impedance of the resonator, the achieved sensitivity would correspond, in the best case, to about 2.5×10^{-19} F in 1-kHz band provided the characteristic impedance would be 75 Ω, or to 5.1×10^{-19} F for 300 Ω. From their data only the voltage at the output of the sensor can be reconstructed ($\approx 0.2\,\mathrm{V_{p-p}}$). Provided the length of the resonator is $\lambda/4$, on the side of the probe the sense voltage should be many times higher. Nevertheless, the design optimised for application in a microscope and higher Q (85) represent an improvement.

Martin *et al.* [9] have made a rather rough estimate of the sensitivity achieved with a Scanning Force Microscope, operated with a voltage applied between a conducting cantilever and the sample, and measuring the force gradient as the probe-sample distance was changed. They obtained a sensitivity 4×10^{-20} F (in unspecified noise band) applying 25 V dc to the tip. At such voltage, the probe/sample distance must be large and the lateral resolution greatly reduced. Higher sensitivity with this kind of microscope can be achieved applying an ac voltage at the frequency of mechanical resonance of the cantilever. However, in air at small distance d, the large capillary forces in adsorbed water films complicate the force measurement.

6 Conclusions

The capacitance measurement methods used in scanning capacitance microscopes offer comparable limiting sensitivities. The highest theoretical sensitivity assumed for videodisk-based instruments was not achieved yet. The published sensitivities are 14 to 220-times lower. At lower frequencies, phase-sensitive measurement of the capacitive current by means of a buffer may give better results than the videodisk-based systems achieved hitherto. Although the microscope described in paper [4] used a buffer with discrete FETs at the input, the estimate of its sensitivity was evidently too optimistic. The sensitivity that can be reached by means of a IUC is about one order of magnitude lower.

All detection methods used hitherto achieve a sensitivity sufficient to reach a lateral resolution limited by the onset of unacceptably large tunnelling current or to operate with applied voltages below 100 mV.

The limiting lateral resolution on conducting surfaces can be as low as 2 nm with tip radius about 7 nm, however at very low contrast.

Acknowledgement: This work was partly supported by the VEGA Grant No. 2/6061/99.

References

[1] C. D. Bugg, P. J. King: *J. Phys.* **E21** (1988) 147
[2] H. P. Kleinknecht, J. R. Sandercock, H. Meier: *Scan. Microsc.* **2** (1988) 1839
[3] C. C. Williams, W. P. Hough, S. A. Rishton: *Appl. Phys. Lett.* **55** (1989) 203
[4] Š. Lányi, J. Török, P. Řehůřek: *Rev. Sci. Instrum.* **65** (1994) 2258
[5] Semiconductor Association, 4300 Stevens Creek Boulevard, Suite 271, San Jose, CA 95129
[6] Y. Huang, C. C. Williams: *J. Vac. Sci. Technol.* **B12** (1994) 369

[7] V. V. Zavyalov, J. S. McMurray, C. C. Williams: *Rev. Sci. Instrum.* **70** (1999) 158
[8] R. C. Palmer, E. J. Denlinger, H. Kawamoto: *RCA Rev.* **43** (1982) 194
[9] Y. Martin, D. W. Abraham, H. K. Wickramasinghe: *Appl. Phys. Lett.* **52** (1988) 1103
[10] Š. Lányi, J. Török: *J. Electrical Eng.* **46** (1995) 126
[11] Š. Lányi, J. Török, P. Řehůřek: *J. Vac. Sci. Technol.* **B14** (1996) 892
[12] Š. Lányi: *Surf. Interface. Anal.* **27** (1999) 348
[13] F. N. Toth, G. C. M. Meijer: *IEEE Trans. Instrum. Meas.* **41** (1992) 1041
[14] Š. Lányi: *Meas. Sci. Technol.* **12** (2001) 1456
[15] Š. Lányi: *J. Electr. Eng.* **52** (2001) 338
[16] H. Tomiye, T. Yao: *Jpn. J. Appl. Phys.* **37** (1998) 3812
[17] Š. Lányi, M. Hruškovic: Electrically Based Microstructural Characterization II, *Mat. Res. Soc. Symp. Proc.* Vol. 500, Materials Research Society, Warrendale, PA 1998
[18] Y. Li, J. N. Nxumalo, D. J. Thomson: *J. Vac. Sci. Technol.* **B16** (1998) 457
[19] T. Tran, D. R. Oliver, D. J. Thomson, G. E. Bridges: *Rev. Sci. Instrum.* **72** (2001) 2618